Temperature-Dependent Spin-Lattice Relaxation of the Nitrogen-Vacancy Spin Triplet in Diamond

M. C. Cambria,[1] A. Norambuena,[2] H. T. Dinani,[3,4] G. Thiering,[5] A. Gardill,[1] I. Kemeny,[1] Y. Li,[1] V. Lordi,[6] Á. Gali,[5,7] J. R. Maze,[8,9] and S. Kolkowitz[1,10,*]

[1]*Department of Physics, University of Wisconsin, Madison, Wisconsin 53706, USA*
[2]*Centro de Optica e Información Cuántica, Universidad Mayor, Camino La Pirámide 5750, Huechuraba, Santiago, Chile*
[3]*Centro de Investigación DAiTA Lab, Facultad de Estudios Interdisciplinarios, Universidad Mayor, Santiago, Chile*
[4]*Escuela Data Science, Facultad de Ciencias, Ingeniería y Tecnología, Universidad Mayor, Santiago, Chile*
[5]*Wigner Research Centre for Physics, P.O. Box 49, 1525 Budapest, Hungary*
[6]*Lawrence Livermore National Laboratory, Livermore, California, 94551, USA*
[7]*Department of Atomic Physics, Institute of Physics, Budapest University of Technology and Economics, Műegyetem rakpart 3., 1111 Budapest, Hungary*
[8]*Instituto de Física, Pontificia Universidad Católica de Chile, Casilla 306, Santiago, Chile*
[9]*Centro de Investigación en Nanotecnología y Materiales Avanzados, Pontificia Universidad Católica de Chile, Santiago, Chile*
[10]*Department of Physics, University of California, Berkeley, California 94720, USA*

(Received 28 September 2022; revised 7 February 2023; accepted 5 June 2023; published 22 June 2023)

Spin-lattice relaxation within the nitrogen-vacancy (NV) center's electronic ground-state spin triplet limits its coherence times, and thereby impacts its performance in quantum applications. We report measurements of the relaxation rates on the NV center's $|m_s = 0\rangle \leftrightarrow |m_s = \pm 1\rangle$ and $|m_s = -1\rangle \leftrightarrow |m_s = +1\rangle$ transitions as a function of temperature from 9 to 474 K in high-purity samples. We show that the temperature dependencies of the rates are reproduced by an *ab initio* theory of Raman scattering due to second-order spin-phonon interactions, and we discuss the applicability of the theory to other spin systems. Using a novel analytical model based on these results, we suggest that the high-temperature behavior of NV spin-lattice relaxation is dominated by interactions with two groups of quasilocalized phonons centered at 68.2(17) and 167(12) meV.

DOI: 10.1103/PhysRevLett.130.256903

Introduction.—The nitrogen-vacancy (NV) center is a point defect in diamond that has become a promising platform for quantum technologies ranging from nanoscale magnetic resonance imaging [1,2] and electric field sensing [3,4] to quantum information processing [5–7]. The NV center owes much of its appeal to its crystalline host, which allows the system to be placed near other materials or integrated into larger devices without the need for trapping or cooling [8,9]. The NV center's solid-state environment also presents significant challenges, however. Interactions between the NV center's electronic spin and phonons in the surrounding crystal lattice drive spin-lattice relaxation [10], also called spin-phonon relaxation [11,12], fundamentally limiting the system's achievable electronic spin coherence times and therefore its performance in quantum applications. Accordingly, several works have explored the temperature dependence of phonon-limited relaxation on the single-quantum transition between the $|m_s = 0\rangle$ and $|m_s = \pm 1\rangle$ levels of the NV's ground-state electronic spin triplet [10,13–15]. Although relaxation on the double-quantum transition between the $|m_s = -1\rangle$ and $|m_s = +1\rangle$ levels also limits coherence times, phonon-limited relaxation on this transition has been less thoroughly studied, leaving maximum achievable NV coherence times unknown for a wide temperature range.

To our knowledge, the only systematic measurements of phonon-limited double-quantum relaxation to date are Refs. [16] and [17]. In Ref. [16], we found that double-quantum relaxation occurs roughly twice as fast as single-quantum relaxation in the phonon-limited regime at room temperature. In Ref. [17], Lin *et al.* present measurements of the single- and double-quantum relaxation rates between room temperature and 600 K, but several discrepancies with prior works suggest that these results cannot be easily generalized to describe NV spin-lattice relaxation in high-purity samples (Fig. S2 in the Supplemental Material [18]). The temperature dependence of phonon-limited double-quantum relaxation has not been characterized below room temperature.

In this Letter, we present measurements of the temperature dependence of the single- and double-quantum relaxation rates of the nitrogen-vacancy center's electronic ground-state spin triplet in high-purity samples from 9 to 474 K. In contrast to prior theoretical understanding [10], we argue that Raman scattering of phonons in the NV center arises mainly due to second-order, rather than first-order, spin-phonon interactions. We develop an *ab initio* framework for calculating the relaxation rates that result from these interactions, and we suggest similar spin

systems that are subject to the same theoretical arguments. Informed by the presence of two vibrational resonances in the NV spin-phonon spectral function, we develop an analytical model of NV spin-lattice relaxation in which transitions are driven by two strongly coupled effective phonon modes at energies of 68.2(17) and 167(12) meV. Additionally, we use our experimental results to calculate the temperature-dependent limits to NV electron spin coherence times imposed by spin-lattice relaxation for superpositions in both the single- and double-quantum subspaces, and we compare these limits to the longest coherence times reported in literature.

Experimental methods.—Figure 1(a) shows the level structure of the NV's ground-state electronic spin triplet, where we abbreviate $|m_s = 0\rangle$ ($|m_s = \pm 1\rangle$) to $|0\rangle$ ($|\pm 1\rangle$). Relaxation on the $|0\rangle \leftrightarrow |\pm 1\rangle$ single-quantum transitions occurs at a common rate Ω; relaxation on the $|-1\rangle \leftrightarrow |+1\rangle$ double-quantum transition occurs at rate γ. Prior studies of phonon-limited spin relaxation in NVs have focused on the lifetime of $|0\rangle$ under the assumption that $|0\rangle$ and either $|-1\rangle$ or $|+1\rangle$ can be considered a qubit and the third level of the spin triplet can be neglected, tacitly assuming $\gamma = 0$ [10,13–15]. These prior works use T_1 to denote the lifetime of $|0\rangle$, which is related to the rates used in this Letter by $T_1 = 1/(3\Omega)$.

The experimental methodology we employ to measure γ and Ω is similar to that of prior works [16,27,28]. Optical polarization and state-selective π pulses enable initialization into any spin state. Following a relaxation time τ, the population in a target state is mapped to $|0\rangle$ and read out optically. Differences between pairs of the measured relaxation curves yield single-exponential decays from which the rates Ω and γ are extracted [Fig. 1(b)] [27,28]. Experiments are conducted using a home built confocal microscope with support for low-temperature (9 K to ambient) and high-temperature (ambient to 474 K) operation modes. A static magnetic field oriented to within 5° of the NV orientation under study is applied with a permanent magnet to lift the $|\pm 1\rangle$ degeneracy by $\Delta_\pm \approx 145$ MHz. Experiments are conducted using two diamond samples with NV concentrations of 1 ppb (sample A) and 10^{-3} ppb (sample B). (See Sec. I in the Supplemental Material [18] for additional experimental details).

Results.—Figure 2 displays measurements of the relaxation rates Ω and γ as functions of temperature between 9 and 474 K for NV ensemble and single NV measurements in samples A and B respectively. Above 125 K, sample-dependent contributions to Ω and γ fall below 10%, indicating that the relaxation rates are dominated by phonons in the diamond lattice, rather than by interactions with other defects. In Ref. [16], we found that $\gamma \approx 2\Omega$ at room temperature. Our results here demonstrate that this factor of 2 is coincidental, as the ratio γ/Ω declines from 2.5 to 1.8 between 200 and 474 K (Fig. S7 in the Supplemental Material [18]).

Prior work has fit the temperature dependence of the single-quantum relaxation rate Ω using an empirical model

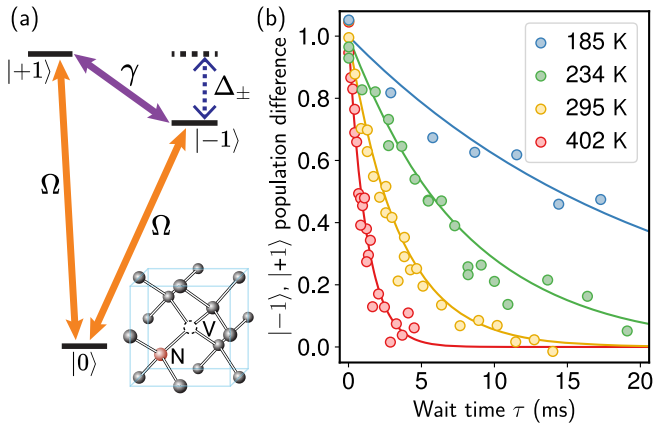

FIG. 1. Phonon-limited spin relaxation in nitrogen-vacancy centers. (a) Level structure of the NV$^-$ ground-state electronic spin triplet. The zero field splitting raises $|\pm 1\rangle$ above $|0\rangle$ by 2.87 GHz at room temperature; a static magnetic field lifts the $|\pm 1\rangle$ degeneracy. Relaxation between $|0\rangle$ and $|\pm 1\rangle$ ($|-1\rangle$ and $|+1\rangle$) occurs at rate Ω (γ). Inset: nitrogen-vacancy defect within a carbon lattice. (b) Effect of temperature on the curves used to extract the relaxation rate γ. Data points show the difference between population in $|+1\rangle$ and $|-1\rangle$ after time τ following initialization in $|+1\rangle$ in sample A. Curves are single-exponential fits with decay rate $2\gamma + \Omega$.

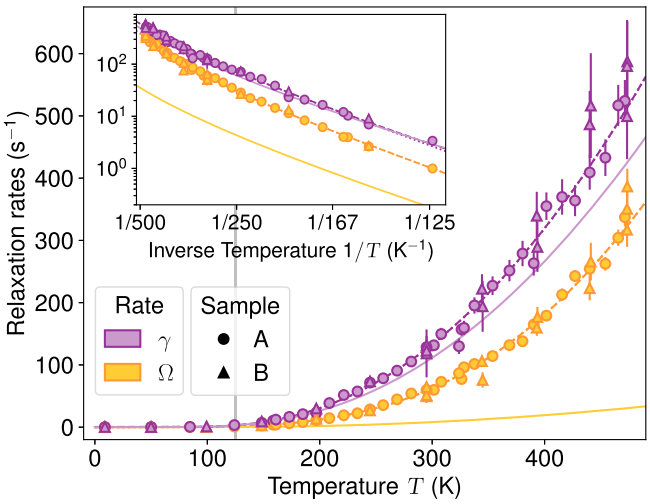

FIG. 2. Temperature dependence of relaxation rates γ and Ω. Error bars are 1σ. Above 125 K (vertical gray line), sample-dependent contributions are below 10%. Darker lines show fit according to the proposed model described by Eqs. (4) and (5), where dotted (dashed) lines include sample-dependent constants for sample A (B). Lighter solid lines show relaxation rates predicted by *ab initio* calculations. See Figs. S4 and S11, and Table S4 in the Supplemental Material [18] for additional plots and full set of data. Inset: semilog plot of relaxation rates versus inverse temperature.

in which two terms chiefly contribute to phonon-limited relaxation: one term that scales in proportion to the phonon occupation number at a specific energy, and a second term that scales with temperature as T^5. The first term has been described as an "Orbach" [13], "Orbach-type" [10,15], or "Orbach-like" [16] process, as the temperature scaling matches that of the standard Orbach process [29,30]. However, the standard Orbach process is unlikely to contribute to spin relaxation in the NV^- center ground state because the nearest excited state that could enable the process is roughly 400 meV above the ground state [31,32], well beyond the phonon cutoff frequency of approximately 165 meV in diamond. The Orbach-like term in prior models has instead been attributed to quasilocalized phonon modes near 73 meV [10]. The interactions giving rise to this term have not been described in detail. The second term has been attributed to Raman scattering of low-energy acoustic phonons that are weakly coupled to the spin via first-order interactions, as described by Walker in Ref. [33]. We argue that Walker's process is negligible in systems like the NV^- ground-state triplet where the spin-phonon interaction strength is much smaller than typical phonon energies. Under this condition, Raman scattering will be driven by second-order, rather than first-order, spin-phonon interactions.

According to Fermi's golden rule, the rate of Raman scattering due to first-order interactions scales quadratically with the square of the first-order interaction strength divided by the energy of the virtual state mediating the transition. Gauging the magnitude of the spin-phonon interaction using the zero field splitting, the first-order interaction strength is roughly $hD\,(\Delta u/a)$, where $D \approx 2.87$ GHz is the NV zero field splitting, Δu is the atomic displacement associated with lattice vibrations, and a is the nearest neighbor distance in diamond. If the nearest excited state is beyond the phonon cutoff frequency, then the virtual state energy is dominated by the phonon energy, $\hbar\omega \sim 50$ meV for acoustic phonons in diamond. Contributions to Raman scattering from first-order interactions will therefore depend quadratically on the quantity $[hD\,(\Delta u/a)]^2/(\hbar\omega)$ for the NV center. On the other hand, the rate of Raman scattering due to second-order interactions scales quadratically with the second-order interaction strength, approximately $hD\,(\Delta u/a)^2$. The ratio between the first- and second-order contributions is on the order of $(2\pi D/\omega)^2 \sim 10^{-7}$ for the NV center, indicating that Raman scattering via first-order interactions can be neglected.

Motivated by these observations, we develop an *ab initio* theory of spin-lattice relaxation where Raman scattering is driven by second-order interactions. The relaxation rate may be expressed as [12]

$$\Gamma = \Gamma_1^{(1)}(T) + \Gamma_1^{(2)}(T) + \Gamma_2^{(1)}(T) + \ldots, \tag{1}$$

where the superscript indicates the order of the spin-phonon interaction (terms with superscript 1 or 2 are linear or quadratic in the atom displacements, respectively) and the subscript indicates the order in perturbation theory. The term $\Gamma_1^{(1)}$ describes single-phonon processes which are only relevant below 1 K for the NV center [34]. At elevated temperatures, relaxation is dominated by Raman scattering of higher energy phonons.

Raman scattering appears as two different second-order terms in Eq. (1): first-order interactions applied to second order in perturbation theory $\Gamma_2^{(1)}$ and second-order interactions applied to first order in perturbation theory $\Gamma_1^{(2)}$. As discussed above, $\Gamma_2^{(1)} \ll \Gamma_1^{(2)}$ for the NV center, and we use Fermi's golden rule to write

$$\Gamma^{(2)}_{1(m_s m_s')}(T) = \frac{2\pi}{\hbar}\sum_{ll'} |V^{ll'}_{m_s m_s'}|^2 [n_l(n_{l'}+1)\delta(\Delta E_-) + n_{l'}(n_l+1)\delta(\Delta E_+)] \tag{2}$$

for spin states $|m_s\rangle$ and $|m_s'\rangle$. Here, $V^{ll'}_{m_s m_s'}$ is the matrix element coupling $|m_s\rangle$ to $|m_s'\rangle$ via phonons l and l', and $\Delta E_\pm = E_{m_s'} \pm (\hbar\omega_l - \hbar\omega_{l'}) - E_{m_s}$ is the energy difference between the final and initial states of the composite system. The mean occupation number for mode l is $n_l = [\exp(\hbar\omega_l/k_B T) - 1]^{-1}$. For high energy phonons, we approximate $\Delta E_\pm \approx \pm(\hbar\omega_l - \hbar\omega_{l'})$ and consider only the diagonal $l = l'$ terms. In the continuum limit Eq. (2) becomes

$$\Gamma^{(2)}_{1(m_s m_s')}(T) = \frac{4\pi}{\hbar}\int_0^\infty d(\hbar\omega) n(\omega)[n(\omega)+1] F^{(2)}_{m_s m_s'}(\hbar\omega, \hbar\omega), \tag{3}$$

where the spectral function $F^{(2)}_{m_s m_s'}(\hbar\omega, \hbar\omega)$ accounts for the phonon density of states and the spin-phonon coupling strengths. For the NV center, we identify $\Gamma^{(2)}_{1(\pm 0)}$ and $\Gamma^{(2)}_{1(+-)}$ as the relaxation rates Ω and γ respectively. (See Sec. VIII of the Supplemental Material [18] for a detailed calculation.)

We obtain the matrix elements $V^{ll}_{m_s m_s'}$ by calculating the derivatives of the NV center's spin-spin induced zero field splitting tensor with respect to atomic displacements. The calculation is performed using a plane wave supercell density functional theory simulation package [35,36] by means of Perdew-Burke-Ernzerhof functional [37]. We approximate the spectral function for a macroscopic diamond by convolving the matrix elements with a normalized Gaussian. The spectral function displays two peaks near 65 and 155 meV (Fig. 3) which are associated with phonon modes that change the positions of the carbon dangling bonds [38] and thereby the spin density distribution.

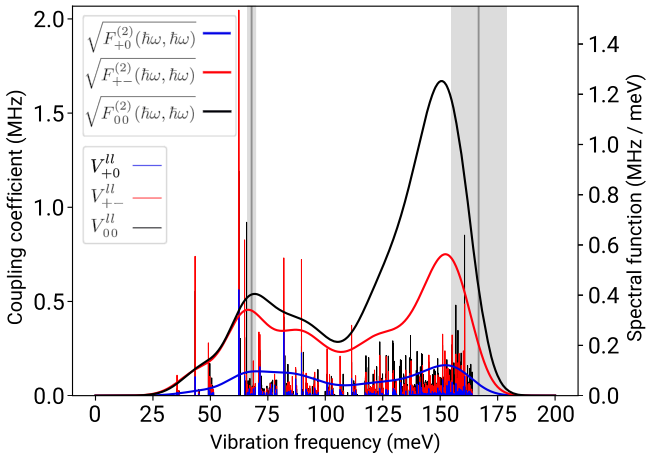

FIG. 3. *Ab initio* second-order spin-phonon coupling coefficients (thin lines) and spectral function (thick curves) for a single NV center in a 512 atom supercell. NV spin-phonon dynamics are characterized by the magnitudes of the matrix elements $\hat{S}_z\hat{S}_+$ (blue), $\hat{S}_+^2$ (red), and $\hat{S}_z^2 - \frac{1}{3}\hat{S}^2$ (black), which cause single-quantum relaxation, double-quantum relaxation, and dephasing respectively. The spectral function displays peaks near the values of 68.2(17) and 167(12) meV extracted from the fit of the two-phonon model to the experimental data (gray lines and $\pm 1\sigma$ intervals).

Evaluating Eq. (3) with the calculated spectral function yields predicted spin-lattice relaxation rates with no free parameters that are in rough quantitative agreement with experiment (lighter solid lines, Fig. 2). Above 125 K, the predicted rates exhibit the same temperature scalings as the measured rates. The double-quantum rate is within 20% of the measured γ, and the single-quantum relaxation rate is approximately 8 times smaller than the measured Ω at room temperature (Fig. S9 in the Supplemental Material [18]). The discrepancy for Ω may be due to the exclusion of mode combinations where $l \neq l'$, as combinations of modes with different symmetries likely yield significant matrix elements for differing spin operators, which drive single-quantum transitions. We leave the calculation of off-diagonal combinations for future work. The *ab initio* calculations validate the intuitive argument made above for the dominance of second-order interactions in Raman scattering for the NV center. The calculated first-order matrix elements are on the order of 100 MHz, resulting in contributions to relaxation that are roughly 6 orders of magnitude smaller than contributions from second-order matrix elements for 50 meV phonons (Fig. S8 in the Supplemental Material [18]).

The double-peaked form of the spectral function $F^{(2)}_{m_s m_s'}(\hbar\omega, \hbar\omega)$ suggests that Eq. (3) can be well approximated by an analytical model of the relaxation rates with two terms corresponding to two effective phonon modes:

$$\Omega(T) = A_1 n_1(n_1+1) + A_2 n_2(n_2+1) + A_3(S), \quad (4)$$

$$\gamma(T) = B_1 n_1(n_1+1) + B_2 n_2(n_2+1) + B_3(S). \quad (5)$$

Here, $n_{1;2} = [\exp(\Delta_{1;2}/k_B T) - 1]^{-1}$ are the mean occupation numbers at characteristic energies $\Delta_{1;2} = \hbar\omega_{1;2}$, $A_{1;2}$ and $B_{1;2}$ are coupling coefficients for the effective modes, and $A_3(S)$ and $B_3(S)$ are sample-dependent constants. Eqs. (4) and (5) provide excellent fits to the experimental data (darker lines in Fig. 2) with residuals that are consistent with purely statistical errors (Fig. S5 in the Supplemental Material [18]). The characteristic energies from the fit are 68.2(17) and 167(12) meV, matching the locations of the peaks in the spectral function. (See Tables S1 and S2 in the Supplemental Material [18] for fit parameters.) Suggestively, the spectral structure of the NV phonon sideband has also been attributed to phonons with the same two characteristic energies as those we extract here [39–41]. At low temperatures, $n_{1;2}(n_{1;2}+1) \approx \exp(-\Delta_{1;2}/k_B T)$. When plotted semilogarithmically versus inverse temperature, scalings of the form $n_{1;2}(n_{1;2}+1)$ therefore appear linear with slope proportional to the activation energy $\Delta_{1;2}$ (Fig. 2 inset).

The model of NV spin-lattice relaxation proposed here differs qualitatively from the empirical models used in prior works to describe the temperature dependence of the single-quantum relaxation rate Ω [10,13,15]. Because $n(n+1) \approx n$ at low temperatures, we suggest that the phenomenological Orbach-like term in prior models corresponds to the first term scaling with $n_1(n_1+1)$ in Eqs. (4) and (5). In contrast to prior models, we attribute the high temperature scaling of the spin-lattice relaxation rates to interactions with a second, higher-energy effective phonon mode leading to a second Orbach-like term, rather than to first-order interactions with low-energy acoustic modes leading to a T^5 term. Although the prior empirical model can be naively extended to provide a good fit to both measured relaxation rates (Fig. S5 in the Supplemental Material [18]), we argue that it is not physically motivated or necessary to include an additional mechanism with a different scaling. Our calculations indicate that the physical process behind the T^5 term in prior models will remain negligible at temperatures up to and exceeding 1000 K, the highest temperature at which the NV center has been coherently manipulated [42]. Given the different asymptotic behavior of the two models, we predict that the prior model of NV spin-lattice relaxation will break down at temperatures beyond those reached experimentally in this Letter. In contrast, we expect that the model proposed here will continue to yield accurate predictions of the relaxation rates at higher temperatures owing to the model's physical underpinnings, and the fact that it already accounts for contributions from the highest energy optical phonons in diamond.

Discussion.—Spin-lattice relaxation is an incoherent process that fundamentally limits achievable coherence times. Much past work with NV centers has neglected

the effect of γ on this limit, thereby overestimating the maximum achievable coherence times [43,44]. Including γ, the relaxation-limited coherence time is

$$T_{2,\max}^{(\mathrm{SQ})} = \frac{2}{3\Omega + \gamma} \tag{6}$$

for superpositions in the $\{|0\rangle, |\pm 1\rangle\}$ single-quantum subspace and

$$T_{2,\max}^{(\mathrm{DQ})} = \frac{1}{\Omega + \gamma}. \tag{7}$$

for superpositions in the $\{|-1\rangle, |+1\rangle\}$ double-quantum subspace [27,28]. Figure 4 shows the relaxation limit in the single-quantum subspace alongside the longest measured values of T_2 at various temperatures reported in the literature [43,45,46]. The best measured coherence times fall short of the calculated limit despite the inclusion of γ. The consistency of the ratio between the measured coherence times and $T_{2,\max}$ in the phonon-limited regime (Fig. 4 inset) suggests that the discrepancy may be due to spin-lattice dephasing, an effect which is not included in Eq. (6) [43]. The similarity of the spectral function line shapes for dephasing (Fig. 3, black curve) and for relaxation (red and blue curves) indicates that these processes may have similar temperature scalings.

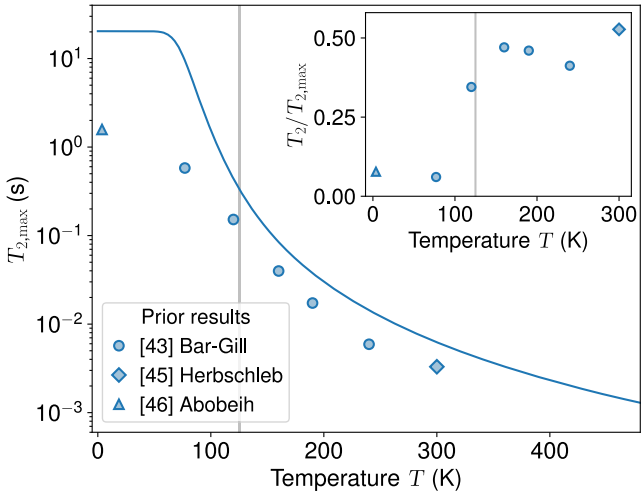

FIG. 4. Temperature dependence of maximum relaxation-limited coherence times. Solid line shows $T_{2,\max}$ in the single-quantum subspace as a function of temperature according to Eq. (6), where Ω and γ are calculated from Eqs. (4) and (5) for sample A. (See Fig. S3 in the Supplemental Material [18] for extended plot.) Vertical gray line at 125 K demarcates the phonon-limited regime. Data points show the longest measured NV coherence times at various temperatures as reported in Refs. [43,45,46]. Inset: ratio of measured coherence times to corresponding limits.

Our results have several implications for future research with NV centers and related systems. Because $T^5 \gg n(n+1)$ at high temperatures, we predict that NV spin-lattice relaxation will be slower than expected based on prior work at temperatures exceeding those accessed in this or previous studies. At 1000 K, we predict relaxation rates several times lower than would have been previously expected. Spin-phonon interaction mitigation schemes such as phononic bandgap engineering [47,48] will likely be ineffective in mitigating the effects of short-wavelength, quasilocalized modes. On the other hand, it may be possible to reduce relaxation by lowering the occupation number of the 167 meV phonon modes in a manner similar to optical cryocooling [49]. In addition, the theoretical model and results presented in this Letter can be generalized to other crystal defects, such as divacancy centers in silicon carbide [50,51] and the boron vacancy center in diamond [52], or to other types of spin systems such as molecular qubits, whose spin-lattice dynamics are under active research [12,53,54]. In Sec. IX of the Supplemental Material [18] we discuss the properties of systems that we expect would make them good candidates for extensions of our model.

Conclusion.—We have presented measurements of the temperature dependence of the NV center's single- and double-quantum relaxation rates in high-purity diamond samples from 9 to 474 K. We argued that Raman scattering in NV centers primarily arises from second-order spin-phonon interactions, and we have developed widely applicable *ab initio* tools for evaluating the relaxation rates that result from these processes. Our *ab initio* calculation of the NV spin-phonon spectral function demonstrates that two distinct groups of quasilocalized modes provide dominant contributions to NV relaxation at high temperatures. Accordingly, we have developed an analytical model of NV spin-lattice relaxation with just two effective phonon modes with characteristic energies of 68.2(17) and 167(12) meV. Finally, we calculated the limits imposed by spin-lattice relaxation on the coherence times of superpositions in the single- and double-quantum subspaces, properly accounting for the NV spin triplet over a wide range of temperatures for the first time.

We gratefully acknowledge Nathalie de Leon and Maxim Vavilov for helpful conversations and feedback on our manuscript. Experimental work, data analysis, and theoretical efforts conducted at UW–Madison were supported by the U.S. Department of Energy, Office of Science, Basic Energy Sciences under Award No. DE-SC0020313. Part of this work by V. L. was performed under the auspices of the U.S. Department of Energy at Lawrence Livermore National Laboratory under Contract No. DE-AC52-07NA27344. A. N. acknowledges financial support from Fondecyt Iniciación No. 11220266. A. G. acknowledges support from the Department of Defense through the National Defense Science and Engineering Graduate

Fellowship (NDSEG) program. Á. G. acknowledges support from the NKFIH in Hungary for the National Excellence Program (Grant No. KKP129866), the Quantum Information National Laboratory (Grant No. 2022-2.1.1-NL-2022-00004), and the EU QuantERA II MAESTRO project and from the European Commission for the QuMicro project (Grant No. 101046911). G. T. was supported by the János Bolyai Research Scholarship of the Hungarian Academy of Sciences. Á. G. and G. T. acknowledge the high-performance computational resources provided by KIFÜ (Governmental Agency for IT Development) Institute of Hungary. J. R. M. acknowledges support from ANID-Fondecyt 1221512.

*kolkowitz@berkeley.edu

[1] D. Rugar, H. Mamin, M. Sherwood, M. Kim, C. Rettner, K. Ohno, and D. Awschalom, Proton magnetic resonance imaging using a nitrogen–vacancy spin sensor, Nat. Nanotechnol. **10**, 120 (2015).

[2] M. Abobeih, J. Randall, C. Bradley, H. Bartling, M. Bakker, M. Degen, M. Markham, D. Twitchen, and T. Taminiau, Atomic-scale imaging of a 27-nuclear-spin cluster using a quantum sensor, Nature (London) **576**, 411 (2019).

[3] T. Iwasaki, W. Naruki, K. Tahara, T. Makino, H. Kato, M. Ogura, D. Takeuchi, S. Yamasaki, and M. Hatano, Direct nanoscale sensing of the internal electric field in operating semiconductor devices using single electron spins, ACS Nano **11**, 1238 (2017).

[4] M. S. Barson, L. M. Oberg, L. P. McGuinness, A. Denisenko, N. B. Manson, J. Wrachtrup, and M. W. Doherty, Nanoscale vector electric field imaging using a single electron spin, Nano Lett. **21**, 2962 (2021).

[5] C. E. Bradley, J. Randall, M. H. Abobeih, R. C. Berrevoets, M. J. Degen, M. A. Bakker, M. Markham, D. J. Twitchen, and T. H. Taminiau, A Ten-Qubit Solid-State Spin Register with Quantum Memory Up to One Minute, Phys. Rev. X **9**, 031045 (2019).

[6] M. Pompili, S. L. Hermans, S. Baier, H. K. Beukers, P. C. Humphreys, R. N. Schouten, R. F. Vermeulen, M. J. Tiggelman, L. dos Santos Martins, B. Dirkse *et al.*, Realization of a multinode quantum network of remote solid-state qubits, Science **372**, 259 (2021).

[7] M. Abobeih, Y. Wang, J. Randall, S. Loenen, C. Bradley, M. Markham, D. Twitchen, B. Terhal, and T. Taminiau, Fault-tolerant operation of a logical qubit in a diamond quantum processor, Nature (London) **606**, 884 (2022).

[8] U. Vool, A. Hamo, G. Varnavides, Y. Wang, T. X. Zhou, N. Kumar, Y. Dovzhenko, Z. Qiu, C. A. Garcia, A. T. Pierce *et al.*, Imaging phonon-mediated hydrodynamic flow in WTe_2, Nat. Phys. **17**, 1216 (2021).

[9] R. N. Patel, T. Schröder, N. Wan, L. Li, S. L. Mouradian, E. H. Chen, and D. R. Englund, Efficient photon coupling from a diamond nitrogen vacancy center by integration with silica fiber, Light **5**, e16032 (2016).

[10] A. Norambuena, E. Muñoz, H. T. Dinani, A. Jarmola, P. Maletinsky, D. Budker, and J. R. Maze, Spin-lattice relaxation of individual solid-state spins, Phys. Rev. B **97**, 094304 (2018).

[11] J. Xu, A. Habib, S. Kumar, F. Wu, R. Sundararaman, and Y. Ping, Spin-phonon relaxation from a universal ab initio density-matrix approach, Nat. Commun. **11**, 2780 (2020).

[12] A. Lunghi, Toward exact predictions of spin-phonon relaxation times: An ab initio implementation of open quantum systems theory, Sci. Adv. **8**, eabn7880 (2022).

[13] D. A. Redman, S. Brown, R. H. Sands, and S. C. Rand, Spin Dynamics and Electronic States of N-*V* Centers in Diamond by EPR and Four-Wave-Mixing Spectroscopy, Phys. Rev. Lett. **67**, 3420 (1991).

[14] S. Takahashi, R. Hanson, J. van Tol, M. S. Sherwin, and D. D. Awschalom, Quenching Spin Decoherence in Diamond through Spin Bath Polarization, Phys. Rev. Lett. **101**, 047601 (2008).

[15] A. Jarmola, V. M. Acosta, K. Jensen, S. Chemerisov, and D. Budker, Temperature- and Magnetic-Field-Dependent Longitudinal Spin Relaxation in Nitrogen-Vacancy Ensembles in Diamond, Phys. Rev. Lett. **108**, 197601 (2012).

[16] M. C. Cambria, A. Gardill, Y. Li, A. Norambuena, J. R. Maze, and S. Kolkowitz, State-dependent phonon-limited spin relaxation of nitrogen-vacancy centers, Phys. Rev. Res. **3**, 013123 (2021).

[17] S. Lin, C. Weng, Y. Yang, J. Zhao, Y. Guo, J. Zhang, L. Lou, W. Zhu, and G. Wang, Temperature-dependent coherence properties of NV ensemble in diamond up to 600 K, Phys. Rev. B **104**, 155430 (2021).

[18] See Supplemental Material at http://link.aps.org/supplemental/10.1103/PhysRevLett.130.256903 for additional experimental and theoretical details, which includes Refs. [19–26].

[19] D. M. Toyli, D. J. Christle, A. Alkauskas, B. B. Buckley, C. G. Van de Walle, and D. D. Awschalom, Measurement and Control of Single Nitrogen-Vacancy Center Spins above 600 K, Phys. Rev. X **2**, 031001 (2012).

[20] C. A. Ryan, J. S. Hodges, and D. G. Cory, Robust Decoupling Techniques to Extend Quantum Coherence in Diamond, Phys. Rev. Lett. **105**, 200402 (2010).

[21] A. M. Souza, G. A. Alvarez, and D. Suter, Robust Dynamical Decoupling for Quantum Computing and Quantum Memory, Phys. Rev. Lett. **106**, 240501 (2011).

[22] B. J. Shields, Q. P. Unterreithmeier, N. P. de Leon, H. Park, and M. D. Lukin, Efficient Readout of a Single Spin State in Diamond via Spin-to-Charge Conversion, Phys. Rev. Lett. **114**, 136402 (2015).

[23] T. H. Taminiau, J. Cramer, T. van der Sar, V. V. Dobrovitski, and R. Hanson, Universal control and error correction in multi-qubit spin registers in diamond, Nat. Nanotechnol. **9**, 171 (2014).

[24] Z. Bodrog and A. Gali, The spin–spin zero-field splitting tensor in the projector-augmented-wave method, J. Phys. Condens. Matter **26**, 015305 (2013).

[25] B. C. Rose, G. Thiering, A. M. Tyryshkin, A. M. Edmonds, M. L. Markham, A. Gali, S. A. Lyon, and N. P. de Leon, Strongly anisotropic spin relaxation in the neutral silicon vacancy center in diamond, Phys. Rev. B **98**, 235140 (2018).

[26] C. Hepp, T. Müller, V. Waselowski, J. N. Becker, B. Pingault, H. Sternschulte, D. Steinmüller-Nethl, A. Gali, J. R. Maze, M. Atatüre *et al.*, Electronic Structure of the Silicon Vacancy Color Center in Diamond, Phys. Rev. Lett. **112**, 036405 (2014).

[27] B. A. Myers, A. Ariyaratne, and A. C. Bleszynski Jayich, Double-Quantum Spin-Relaxation Limits to Coherence of Near-Surface Nitrogen-Vacancy Centers, Phys. Rev. Lett. **118**, 197201 (2017).
[28] A. Gardill, M. C. Cambria, and S. Kolkowitz, Fast Relaxation on Qutrit Transitions of Nitrogen-Vacancy Centers in Nanodiamonds, Phys. Rev. Appl. **13**, 034010 (2020).
[29] C. Finn, R. Orbach, and W. Wolf, Spin-lattice relaxation in cerium magnesium nitrate at liquid helium temperature: A new process, Proc. Phys. Soc. **77**, 261 (1961).
[30] R. Orbach, Spin-lattice relaxation in rare-earth salts, Proc. R. Soc. A **264**, 458 (1961).
[31] Á. Gali, Ab initio theory of the nitrogen-vacancy center in diamond, Nanophotonics **8**, 1907 (2019).
[32] S. A. Wolf, I. Meirzada, G. Haim, and N. Bar-Gill, Nitrogen-Vacancy Singlet-Manifold Ionization Energy, Phys. Rev. Appl. **19**, 034076 (2023).
[33] M. Walker, A T^5 spin–lattice relaxation rate for non-Kramers ions, Can. J. Phys. **46**, 1347 (1968).
[34] J. Gugler, T. Astner, A. Angerer, J. Schmiedmayer, J. Majer, and P. Mohn, Ab initio calculation of the spin lattice relaxation time T_1 for nitrogen-vacancy centers in diamond, Phys. Rev. B **98**, 214442 (2018).
[35] G. Kresse and J. Hafner, Ab initio molecular dynamics for liquid metals, Phys. Rev. B **47**, 558 (1993).
[36] G. Kresse and J. Furthmüller, Efficient iterative schemes for ab initio total-energy calculations using a plane-wave basis set, Phys. Rev. B **54**, 11169 (1996).
[37] J. P. Perdew, K. Burke, and M. Ernzerhof, Generalized Gradient Approximation Made Simple, Phys. Rev. Lett. **77**, 3865 (1996).
[38] J. Zhang, C.-Z. Wang, Z. Z. Zhu, and V. V. Dobrovitski, Vibrational modes and lattice distortion of a nitrogen-vacancy center in diamond from first-principles calculations, Phys. Rev. B **84**, 035211 (2011).
[39] G. Davies, Vibronic spectra in diamond, J. Phys. C **7**, 3797 (1974).
[40] A. Collins, M. Stanley, and G. Woods, Nitrogen isotope effects in synthetic diamonds, J. Phys. D **20**, 969 (1987).
[41] A. Alkauskas, B. B. Buckley, D. D. Awschalom, and C. G. Van de Walle, First-principles theory of the luminescence lineshape for the triplet transition in diamond NV centres, New J. Phys. **16**, 073026 (2014).
[42] G.-Q. Liu, X. Feng, N. Wang, Q. Li, and R.-B. Liu, Coherent quantum control of nitrogen-vacancy center spins near 1000 kelvin, Nat. Commun. **10**, 1344 (2019).
[43] N. Bar-Gill, L. M. Pham, A. Jarmola, D. Budker, and R. L. Walsworth, Solid-state electronic spin coherence time approaching one second, Nat. Commun. **4**, 1743 (2013).
[44] B. Naydenov, F. Dolde, L. T. Hall, C. Shin, H. Fedder, L. C. L. Hollenberg, F. Jelezko, and J. Wrachtrup, Dynamical decoupling of a single-electron spin at room temperature, Phys. Rev. B **83**, 081201(R) (2011).
[45] E. Herbschleb, H. Kato, Y. Maruyama, T. Danjo, T. Makino, S. Yamasaki, I. Ohki, K. Hayashi, H. Morishita, M. Fujiwara *et al.*, Ultra-long coherence times amongst room-temperature solid-state spins, Nat. Commun. **10**, 3766 (2019).
[46] M. H. Abobeih, J. Cramer, M. A. Bakker, N. Kalb, M. Markham, D. J. Twitchen, and T. H. Taminiau, One-second coherence for a single electron spin coupled to a multi-qubit nuclear-spin environment, Nat. Commun. **9**, 2552 (2018).
[47] J. V. Cady, O. Michel, K. W. Lee, R. N. Patel, C. J. Sarabalis, A. H. Safavi-Naeini, and A. C. B. Jayich, Diamond optomechanical crystals with embedded nitrogen-vacancy centers, Quantum Sci. Technol. **4**, 024009 (2019).
[48] G. Wolfowicz, F. J. Heremans, C. P. Anderson, S. Kanai, H. Seo, A. Gali, G. Galli, and D. D. Awschalom, Quantum guidelines for solid-state spin defects, Nat. Rev. Mater. **6**, 906 (2021).
[49] M. Kern, J. Jeske, D. W. M. Lau, A. D. Greentree, F. Jelezko, and J. Twamley, Optical cryocooling of diamond, Phys. Rev. B **95**, 235306 (2017).
[50] N. T. Son, P. Carlsson, J. ul Hassan, E. Janzén, T. Umeda, J. Isoya, A. Gali, M. Bockstedte, N. Morishita, T. Ohshima, and H. Itoh, Divacancy in 4H-SiC, Phys. Rev. Lett. **96**, 055501 (2006).
[51] W. F. Koehl, B. B. Buckley, F. J. Heremans, G. Calusine, and D. D. Awschalom, Room temperature coherent control of defect spin qubits in silicon carbide, Nature (London) **479**, 84 (2011).
[52] T. Umeda, K. Watanabe, H. Hara, H. Sumiya, S. Onoda, A. Uedono, I. Chuprina, P. Siyushev, F. Jelezko, J. Wrachtrup *et al.*, Negatively charged boron vacancy center in diamond, Phys. Rev. B **105**, 165201 (2022).
[53] L. Escalera-Moreno, N. Suaud, A. Gaita-Arino, and E. Coronado, Determining key local vibrations in the relaxation of molecular spin qubits and single-molecule magnets, J. Phys. Chem. Lett. **8**, 1695 (2017).
[54] A. Lunghi, F. Totti, R. Sessoli, and S. Sanvito, The role of anharmonic phonons in under-barrier spin relaxation of single molecule magnets, Nat. Commun. **8**, 14620 (2017).